Nano Res (2009) 2: 713–721
DOI 10.1007/s12274-009-9075-y
Research Article

Magnesium Microspheres and Nanospheres: Morphology-Controlled Synthesis and Application in Mg/MnO_2 Batteries

Chunsheng Li, Fangyi Cheng, Weiqiang Ji, Zhanliang Tao, and Jun Chen (✉)

Institute of New Energy Material Chemistry and Engineering Research Center of Energy Storage and Conversion (Ministry of Education), Nankai University, Tianjin 300071, China

Received: 27 April 2009 / Revised: 28 June 2009 / Accepted: 23 July 2009

ABSTRACT

In this paper, we report on the morphology-controlled synthesis of magnesium micro/nanospheres and their electrochemical performance as the anode of primary Mg/MnO_2 batteries. Mg micro/nanoscale materials with controllable shapes have been prepared via a conventional vapor-transport method under an inert atmosphere by adjusting the deposition temperatures. Extensive analysis techniques including SEM, XRD, TEM/HRTEM, and Brunauer–Emmett–Teller (BET) were carried out to characterize the as-obtained samples. The results show that the Mg samples are microspheres or micro/nanospheres with specific surface areas of 0.61–1.92 m^2/g. The electrochemical properties of the as-prepared Mg and commercial Mg powders were further studied in terms of their linear sweep voltammograms, impedance spectra, and discharge capability. By comparing the performance of different inhibitors in electrolytes, it was found that $NaNO_2$ (2.6 mol/L) as an inhibitor in the $Mg(NO_3)_2$ (2.6 mol/L) electrolyte affords a Mg electrode with high current density and low corrosion rate. In particular, the Mg sample consisting of microspheres with a diameter of 1.5–3.0 μm and nanospheres with a diameter of 50–150 nm exhibited superior electrode properties including negative initial potential (–1.08 V), high current density (163 mA/cm^2), low apparent activation energy (5.1 kJ/mol), and high discharge specific capacity (784 mAh/g). The mixture of Mg nanospheres and microspheres is promising for application in primary Mg/MnO_2 batteries because of the sufficient contact with the electrolyte and greatly reduced charge transfer impedance and polarization.

KEYWORDS

Magnesium, micro/nanospheres, vapor-transport method, primary Mg/MnO_2 batteries

Introduction

Magnesium (Mg), which possesses the outstanding merits of plentiful resources in the earth's crust, environmental friendliness, and low cost, has attracted much interest in the fields of electrochemical energy storage and conversion such as for primary and secondary batteries [1–3]. For primary batteries, Mg is used as the anode material in various cell systems such as Mg/MnO_2, Mg/air, Mg/CuCl, and Mg/AgCl batteries [4–10]. Among these Mg-based batteries, the Mg/MnO_2 battery displays the virtues of a Mg anode with low redox potential (–2.36 V vs

Address correspondence to chenabc@nankai.edu.cn

SHE) and high specific electrochemical capacity (2.2 Ah/g), high theoretical energy density, and long shelf-life compared with that of traditional Zn/MnO_2 batteries [6–9]. Although great progress has been made during the past few decades, problems still remain for Mg/MnO_2 batteries such as low anode utilization of Mg sheet material, low actual energy density, and high cost, which hinder its widespread application in the consumer market. The scientific issues associated with these practical problems can be grouped into three categories: low kinetics of active materials, passivation of the Mg anode by the formation of a $Mg(OH)_2$ film, and an unsuitable electrolyte leading to a high corrosion rate of the anode. Therefore, enhancing the electrochemical activity of the electrode materials (i.e., Mg and MnO_2) and using an appropriate electrolyte can greatly improve the overall performance of the Mg/MnO_2 battery.

A few studies have been carried out in recent years to solve the problems facing Mg/MnO_2 batteries. Renuka's group employed an aluminium-zinc-magnesium alloy sheet as anode and birnessite-type MnO_2 as the cathode to assemble a Mg/MnO_2 battery with an electrolyte composed of a mixture of $Mg(ClO_4)_2$ and $BaCrO_4$ [8]. Vuorilehto tested electrolytes containing various chloride salts in water-activated Mg/MnO_2 batteries, and found that batteries with KCl or NaCl displayed similar discharge times in an atmospheric chamber [9]. In our previous work, we have shown that the morphology of Mg nano/mesoscale materials has a great impact on the current densities of Mg electrodes and the energy densities of Mg/air batteries using an electrolyte of $Mg(NO_3)_2$ and $NaNO_2$ [5]. We have also demonstrated that one-dimensional (1-D) gamma (γ)-MnO_2 nanostructures prepared by a hydrothermal method exhibit a superior discharge performance as the cathode material in both alkaline primary Zn/MnO_2 and rechargeable Li/MnO_2 batteries [11, 12]. However, the major issues yet to be resolved for Mg/MnO_2 batteries are the anodic corrosion and electrode polarization. Therefore, it is necessary to pursue a novel electrolyte with effective inhibitors, and further investigate the effect of the shape of the electrode materials on the battery performance.

In this paper, we focus on the morphology-controlled synthesis of Mg micro/nanostructures and their application in Mg/MnO_2 primary batteries. Three key points have been addressed. First, Mg micro/nanoscale spheres have been successfully prepared via a conventional vapor-transport method by adjusting the deposition temperatures. Second, a moderate concentration of $NaNO_2$ as an inhibitor in the $Mg(NO_3)_2$ electrolyte is employed in order to satisfy the strict requirements of low corrosion rate and low anodic polarization. Third, the as-prepared Mg micro/nanospheres, γ-MnO_2 nanowires, and the optimized electrolyte are used to assemble Mg/MnO_2 batteries. Electrochemical investigations revealed that the batteries assembled with the Mg micro/nanostructures demonstrate superior performance to that of commercial Mg powders in terms of plateau potential, current density, activation energy, and specific discharge capacity. The present study should promote the application of Mg micro/nanostructures in fabricating Mg/MnO_2 batteries with high energy and high power.

1. Experimental

1.1 Sample preparation

For the preparation of Mg micro/nanoscale materials, the vapor-deposition apparatus the experimental procedures, and parameters were similar to that used in our previous work at an evaporation temperature of 825 °C in argon atmosphere [13], except for changing the deposition temperature at 240, 270, and 300 °C on the substrate, which was a stainless steel screen mesh (material: 316L) for collecting the depositing samples. Detailed experimental parameters are summarized in Table 1. γ-MnO_2 nanowires were prepared through a hydrothermal method by heating a solution of $MnSO_4$ and $(NH_4)_2S_2O_8$ at 90 °C for 24 h [11]. The black wool-like products were collected by centrifugation, washed several times with deionized water and ethanol, and vacuum dried at 80 °C for 8 h. The treatment of the MnO_2 was similar to the method reported previously [14].

The morphology and structure of the as-prepared Mg and MnO_2 samples were characterized by

Table 1 Experimental parameters for the Mg products. All samples were obtained by heating commercial Mg powders at 825 °C for 2 h with the same flow rate of 800 cm^3/min

Sample	Deposition temperature (°C)	Main morphology	Specific surface area (m^2/g)
1	240	Microspheres (1.0–5.0 μm)	0.73
2	270	Microspheres (3.0–6.0 μm)	0.61
3	300	Microspheres (1.5–3.0 μm) & nanospheres (50–150 nm)	1.92

scanning electron microscopy (SEM) (Philips XL-30 and JEOL JSM-6700F field emission), transmission electron microscopy (TEM)/high-resolution TEM (HRTEM) (FEI Tecnai G2 F20 S-Twin, 200 kV), and powder X-ray diffraction (XRD) (Rigaku D/max-2500 X-ray generator, Cu K_α radiation). The structure refinement of the XRD profiles was performed by the Rietveld method using a multipurpose pattern-fitting program RIETAN-2000 [15]. The Brunauer–Emmett–Teller (BET) specific surface areas of the samples were determined by measuring N_2 adsorption isotherms at the temperature of liquid nitrogen (BELSORP-mini II, Bel Japan Inc.).

Magnesium electrodes were prepared under the protection of an argon atmosphere in a glove box (Mikrouna China Universal 2240/750) with a mixture of active materials (as-prepared Mg products and commercial Mg powders), Vulcan XC-72 carbon (Cabot), and polytetrafluoroethylene (PTFE) binder with a mass ratio of Mg: carbon: PTFE = 65:25:10. The electrochemical properties of the electrodes were measured with a Parstat 2273 potentiostat/galvanostat analyzer (AMETEK Co.) in a three-electrode cell composed of a Mg working electrode, a platinum counter electrode, and Ag/AgCl (KCl saturated) as a reference electrode [5]. The impedance spectra were analyzed by fitting to an equivalent circuit using the ZSimpWin software. As listed in Table 2, various electrolytes were selected to study the performances of the Mg anode.

Table 2 Summary of composition of different electrolytes for Mg electrodes

Electrolyte	Composition
a	0.65 mol/L $Mg(ClO_4)_2$ and 0.01 mol/L $Ba(CrO_4)_2$
b	2.6 mol/L $Mg(NO_3)_2$ and 3.6 mol/L $NaNO_2$
c	1.8 mol/L $Mg(ClO_4)_2$ and 0.05 mol/L LiCl
d	2.6 mol/L $Mg(NO_3)_2$ and 4.6 mol/L $NaNO_2$
e	2.6 mol/L $Mg(NO_3)_2$ and 2.6 mol/L $NaNO_2$

The laboratory-made CR2032 Mg/MnO_2 coin-cells were composed of a Mg anode, a γ-MnO_2 cathode, and a separator. The MnO_2 electrodes contained 80 wt% of the as-synthesized γ-MnO_2 nanowires (see Fig. S-1 in the Electronic Supplementary Material (ESM)), 10 wt% Vulcan XC-72 carbon, 8 wt% PTFE binder, and 2 wt% $Mg(OH)_2$. The electrodes were dried at 80 °C for 8 h and cut into a disk with a diameter of 16 mm. The electrolyte was a mixture of $Mg(NO_3)_2$ and $NaNO_2$. The discharge performances were measured on the LAND CT2001A charge–discharge device to an end voltage of 0.8 V at a constant current density of 25 mA/g at 25 °C.

2. Results and discussion

2.1 Characterization of the as-synthesized Mg materials

Figure 1 shows typical SEM images of Mg products prepared by a vapor deposition process with different deposition temperatures (240–300 °C). Figures 1(a) and 1(b) display representative SEM micrographs of sample 1 obtained at a deposition temperature of 240 °C. It can be clearly seen that uniform Mg microspheres were distributed homogeneously on both the surface and the holes of the screen mesh substrate. The higher-magnification SEM image in Fig. 1(b) reveals that the diameter of the as-prepared microspheres is approximately 1.0–5.0 μm. After increasing the deposition temperature to 270 °C without changing any other experimental conditions, a thick layer of Mg microspheres with different size (sample 2) covered the whole surface of the substrate, indicating a high yield of spheres (Fig. 1(c)). The diameters of these spheres were in the range 3.0–6.0 μm (Fig. 1(d)). More interestingly, a mixture of Mg micro/nanospheres (sample 3) was obtained at

a higher deposition temperature of 300 °C, as shown in Fig. 1(e). The diameter of the microspheres with smooth surfaces was only 1.5–3.0 μm, and abundant nanospheres with diameters of 50–150 nm were found on the surface of Mg microspheres (Fig. 1(f)). The SEM analyses show that different deposition temperatures afforded Mg products with different size, and that a mixture of Mg micro/nanospheres was formed by deposition at higher temperature.

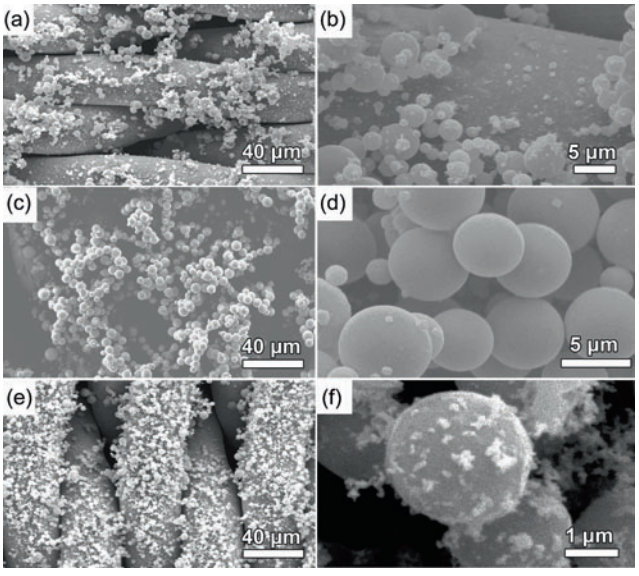

Figure 1 SEM images of the vapor-deposited Mg micro/nanoscale materials for different deposition temperatures: (a), (b) 240 °C (sample 1); (c), (d) 270 °C (sample 2); (e), (f) 300 °C (sample 3)

The crystallographic structures of the as-prepared products were characterized by powder XRD (ESM, Fig. S-2). A representative Rietveld refinement profile of Mg microspheres with the diameter of 1.0 –5.0 μm (sample 1) is shown in Fig. 2, which reveals that the crystal structure of the as-prepared sample is hexagonal close packed (hcp) Mg (ICDD-JCPDS Card No. 35-0821, space group *P63/mmc* (No. 194)). The determined cell parameters (ESM, Table S-1) are very close to the standard values, confirming the identity of the product. To clarify whether a MgO film is coated on the microspheres, we made a further investigation of the Mg microspheres by TEM/HRTEM. Figures 2(b) and 2(c) show the TEM/HRTEM micrographs of Mg microspheres (sample 3). The TEM image revealed that Mg microspheres and nanoparticles had diameters of 1.2–1.5 μm and 25–150 nm, respectively. The HRTEM images (Fig. 2(c)) indicated the good crystallinity of the edge of the Mg microsphere, which was confirmed by the lattice fringes with an interplanar spacing of 0.24 nm corresponding to the spacing of neighboring (101) planes. A very thin (approximately 0.35 nm) coating of an amorphous layer was observed on the surface of the microsphere. This thin layer probably results from the formation of MgO during the TEM sample preparation process. It should be noted that the oxidation layer could be also caused by oxygen and/or water from the electrolyte or cathode materials. The MgO film may have the following three effects [16–19]. First, the formation of MgO provides a protective coating to prevent further oxidation of Mg during the preparation of the anode electrode. Second, the coating may hinder the agglomeration of Mg micro/nanoscale products. Third, polycrystalline

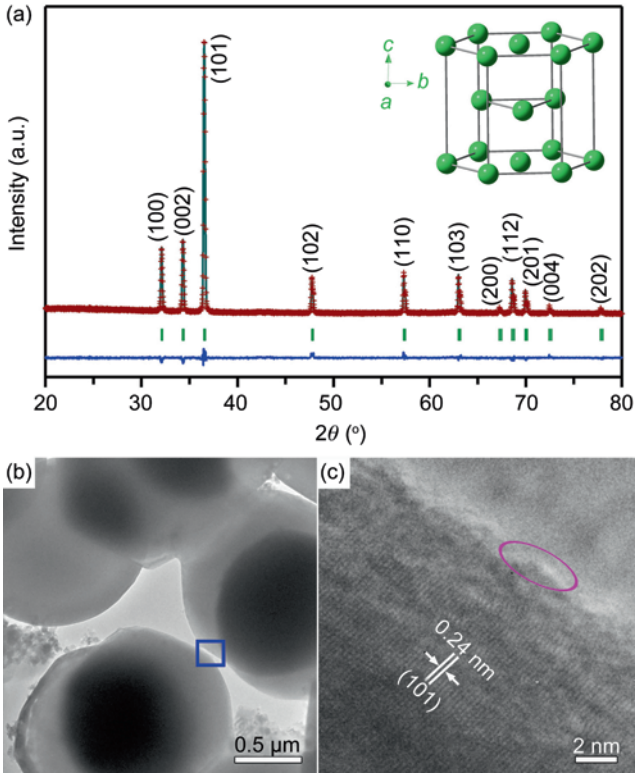

Figure 2 (a) Rietveld analysis of Mg microspheres (sample 1) with the observed (red crosses), calculated (green line), and the difference (blue solid line at the bottom) profiles. The short green vertical bars indicate the peak positions of all possible reflections which are indexed by the corresponding (*hkl*) indices. The inset at the top right corner shows the hcp structure of Mg viewed along slightly downwards tilted axes *a*. (b) TEM image of the as-prepared Mg (sample 3). (c) HRTEM image enclosed in the blue square of (b), indicating the crystallization quality of the product. The pink ellipse in (c) indicates the edge of Mg microsphere with a very thin coating

MgO can exhibit catalytic performance for adsorbed gases on the electrode owing to the crystal shapes and a high ratio of coordinatively unsaturated edge/corner surface sites. Further studies of the mechanism of the catalytic action of MgO in battery systems will be performed in the near future.

2.2 Electrochemical measurements

One of the main problems of Mg/MnO_2 batteries in their practical applications is the formation of a passivating layer on the surface of the Mg anode, which causes an increase in the internal resistance and the loss of the electrochemical potential in most electrolytes [7, 9]. Since this affects the electrochemical performance to a great extent, an ideal electrolyte in these batteries should be able to inhibit the growth of the resistive oxide film, and reduce hydrogen evolution at the Mg electrode. Therefore, various commercial electrolytes for Mg/MnO_2 were screened for their ability to satisfy this requirement.

Figure 3(a) shows the linear sweep voltammograms (LSV) of Mg anodes made from commercial Mg powders (purity: 99.8 %) in three different electrolytes. The current densities of the Mg anodes all increased when the potential was scanned from –1.5 to –0.5 V vs Ag/AgCl–KCl (saturated) at a sweep rate of 20 mV/s. For a $Mg(ClO_4)_2/Ba(CrO_4)_2$ electrolyte (**1**), the potentiostatic anodic polarization curves increased sharply within the electrochemical window, and the current density reached approximately 80 mA/cm^2 at a potential of –0.5 V. However, dense bubbles were seen on the electrode under open circuit conditions in the electrolyte (**a**), which indicates rapid corrosion. The capacity loss of Mg is mainly due to the corrosion with the evolution of hydrogen gas and the fast removal of water from the electrolyte [9, 20]. The corresponding reaction for the corrosion of Mg anode can be described by Eq. (1):

$$Mg + 2H_2O \longrightarrow Mg(OH)_2 + H_2\uparrow \quad (1)$$

With a $Mg(ClO_4)_2/LiCl$ electrolyte(**b**), a flow of H_2 bubbles was immediately generated from the electrode and a coherent film of $Mg(OH)_2$ covered the surface of anode. This film is insoluble in neutral solution and thus reduces the exposure of fresh magnesium to the electrolyte. In addition, the hydrogen release unquestionably causes the self-discharge reaction and the increase of internal pressure which directly leads to the leakage of the electrolyte in a sealed system. Fortunately, few bubbles are formed during the discharge process for the $Mg(NO_3)_2/NaNO_2$ electrolyte (**c**), implying a low speed of corrosion. Since the Mg electrode in the mixed electrolyte of $Mg(NO_3)_2$ and $NaNO_2$ exhibits a low open-circuit corrosion and low anodic polarization, we adopted this electrolyte for use in Mg/air batteries and investigated the effect of

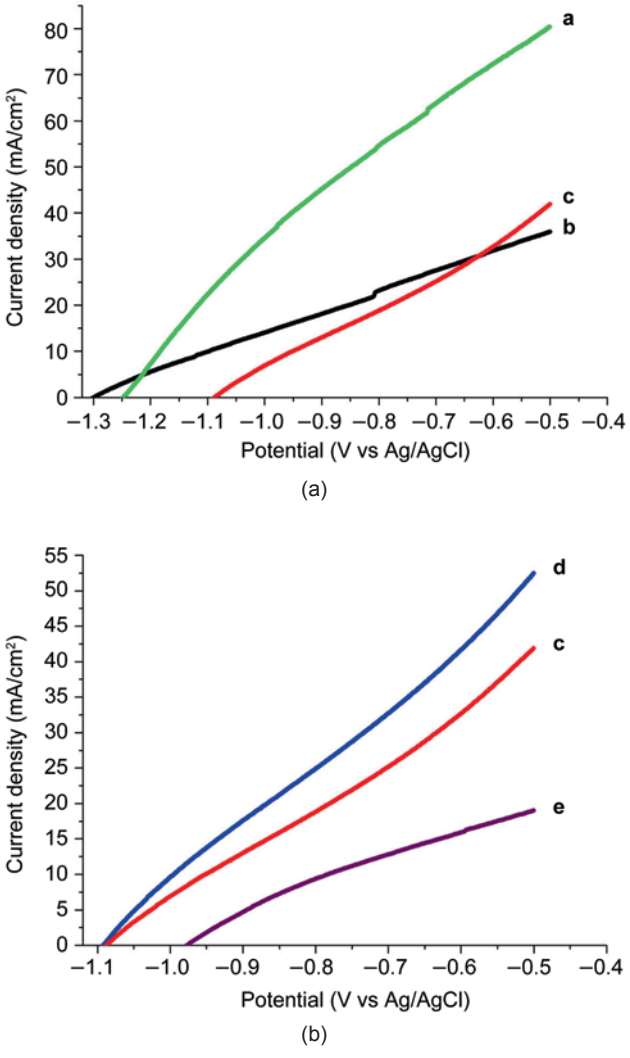

Figure 3 (a) LSV of Mg anodes made from commercial Mg powders (99.8 %) in three kinds of electrolytes: (**a**) 0.65 mol/L $Mg(ClO_4)_2$ and 0.01 mol/L $Ba(CrO_4)_2$; (**b**) 1.8 mol/L $Mg(ClO_4)_2$ and 0.05 mol/L LiCl; (**c**) 2.6 mol/L $Mg(NO_3)_2$ and 3.6 mol/L $NaNO_2$. (b) LSV of Mg electrodes at different concentrations of $NaNO_2$ inhibitor: (**d**) 2.6 mol/L $Mg(NO_3)_2$ and 2.6 mol/L $NaNO_2$, and (**e**) 2.6 mol/L $Mg(NO_3)_2$ and 1.6 mol/L $NaNO_2$. Potential range: −1.50 to −0.5 V vs Ag/AgCl (saturated with KCl), scan rate: 20 mV/s

different Mg products on the discharge properties.

In order to provide a long operating life, an inhibitor in the electrolyte is needed to minimize the corrosion of the anode [8]. In the mixed solution of $Mg(NO_3)_2$ and $NaNO_2$, the $NaNO_2$ acts as an excellent inhibitor to avoid self-discharge of the anode [10], which is especially critical for Mg materials. To find the optimal concentration of the $NaNO_2$ inhibitor, the electrode properties were further investigated. Figure 3(b) shows the LSV of Mg anodes in electrolytes with different concentrations of $NaNO_2$ (1.6, 2.6, and 3.6 mol/L) and the same concentration of $Mg(NO_3)_2$. During the anodic scan, all the current densities of anodic dissolution gradually increase over the potential range –1.3 to –0.5 V at a scan rate of 20 mV/s. In Fig. 3(b), both the initial potentials and the anodic current densities showed differences between electrolytes. Electrolyte (**d**) (2.6 mol/L $NaNO_2$) and electrolyte (**c**) (3.6 mol/L $NaNO_2$) have the same starting potential of –1.08 V, but electrolyte (**d**) provides a higher current density (52 mA/cm^2) at –0.5 V. When the concentration of $NaNO_2$ is 1.6 mol/L (Fig. 3(b), electrolyte (**e**) an obvious decrease in electrode performance was observed. Furthermore, the current density for electrolyte (**e**) was halved in comparison to that for electrolyte (**c**). These results clearly suggest that moderate concentrations of $NaNO_2$ are suitable as an inhibitor for the Mg electrode. In the following, electrolyte (**d**) (a mixture of 2.6 mol/L $Mg(NO_3)_2$ and 2.6 mol/L $NaNO_2$) was used to assemble Mg/MnO_2 batteries.

Figure 4 shows the polarization curves for the as-synthesized Mg electrodes (samples 1–3 and commercial Mg powders) using the mixture of $Mg(NO_3)_2$ (2.6 mol/L) and $NaNO_2$ (2.6 mol/L) as the electrolyte. The potentials of the Mg micro/nanomaterials were more negative than that of commercial Mg. As for the current density of these samples, the vapor-deposited Mg samples possessed superior performance to that of commercial Mg powders. The values of the current density decreased in the order sample 3 > sample 1 > sample 2, which coincides with the reverse sequence of the average diameters of products and the specific surface areas (Table 1). Consequently, the as-obtained Mg can effectively improve the electrode performance,

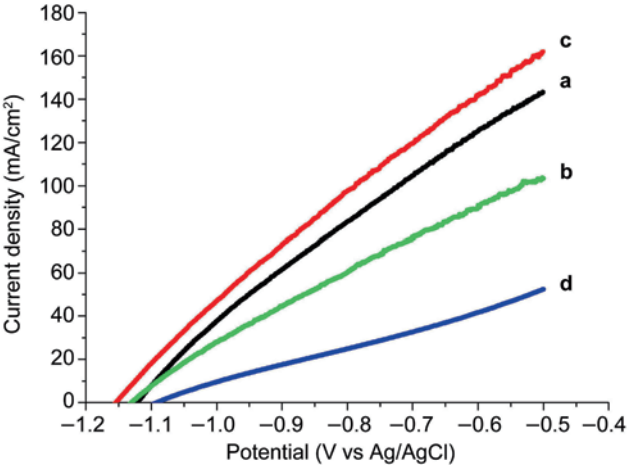

Figure 4 LSV of different Mg electrodes in an electrolyte of 2.6 mol/L $Mg(NO_3)_2$ and 2.6 mol/L $NaNO_2$: (**a**) sample 1, (**b**) sample 2, (**c**) sample 3, (**d**) commercial Mg powder. Sweep rate is fixed at 20 mV/s

especially for a mixture (sample 3) composed of small microspheres (diameters: 1.5–3.0 μm) and nanospheres (diameters: 50–150 nm). This observed decrease in the electrode polarization when the micro/nanoscale composite (sample 3) is used is because it provides the most effective contact with the solution.

In order to study the polarization and kinetics of the Mg microspheres and the micro/nanoscale mixture, the activation energies were evaluated by electrochemical impedance spectroscopy (EIS). Figure 5 shows typical EIS plots of samples 1, 2, 3, and commercial Mg powders at different temperatures under open-circuit conditions. The impedance curves of the four electrodes have a similar profile with a semicircle in the high-frequency region and a straight line in the low-frequency region. The decrease of the depressed semicircles at high frequency with temperature (in the range 304–313 K) reflects the decrease of the resistance of the Mg electrodes. The values of the charge transfer impedance (R_{ct}) were obtained by fitting to an equivalent circuit using the ZSimpWin software (Fig. S-3 and Table S-2 in the ESM) [21]. The apparent activation energies (E_a) of Mg can be calculated from the Arrhenius relation (Eq. (**2**)):

$$\ln(T/R_{ct}) = -E_a/RT + \ln A' \quad (2)$$

where T is the absolute temperature, R_{ct} is the charge transfer impedance determined from the equivalent

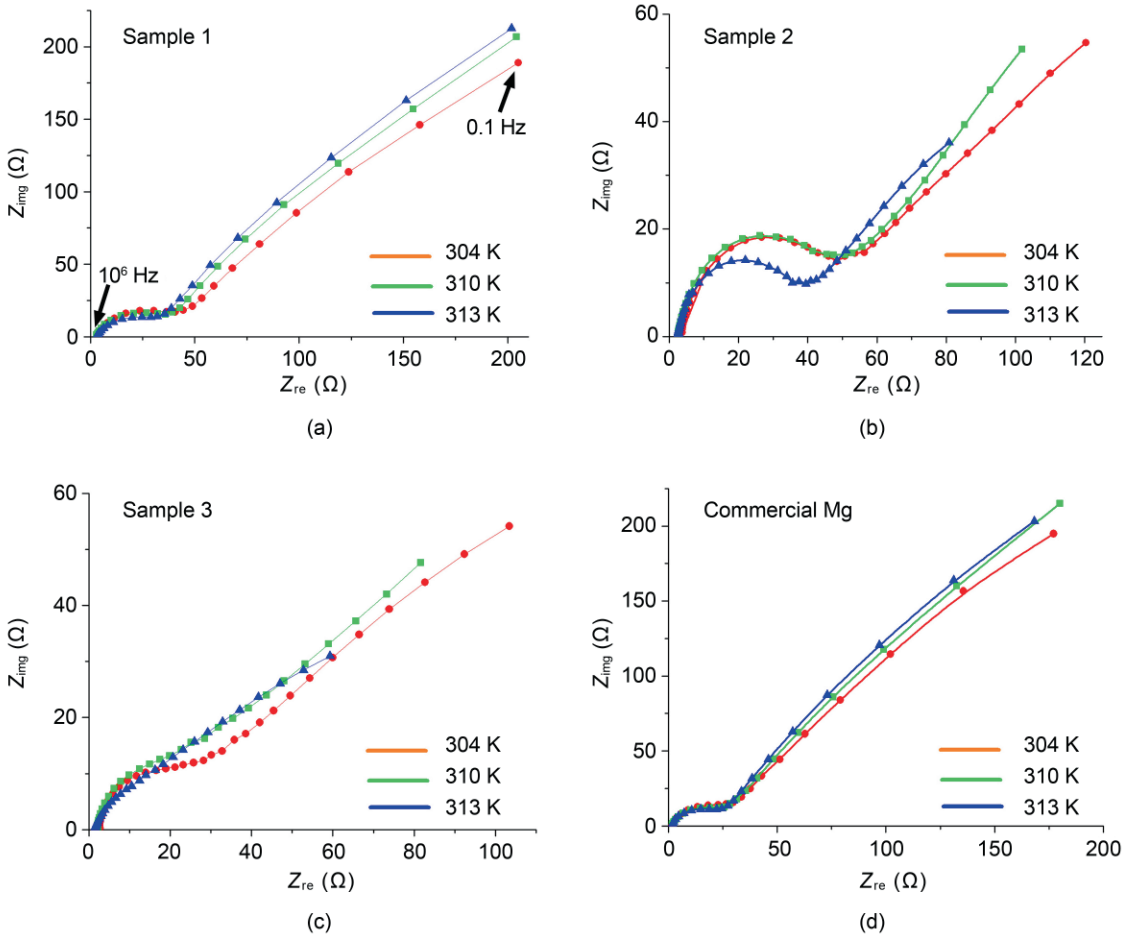

Figure 5 EIS curves of four Mg samples at different temperatures under the open-circuit condition: (a) sample 1, (b) sample 2, (c) sample 3, and (d) commercial Mg powder. The EIS was measured in the frequency range from 1×10^6 to 0.1 Hz

circuit, R is the gas constant, and A' is a temperature-independent coefficient. An Arrhenius plot of $\ln(T/R_{ct})$ as a function of $1000/T$ is shown in Fig. S-4 in the ESM. According to Eq. (2), the activation energies of samples 1, 2, 3, and commercial Mg are 9.1, 14.3, 5.1, and 49.7 kJ/mol, respectively. It is noted that the Mg micro/nanosphere mixture (sample 3) has the lowest apparent activation energy, indicating that the mixed nano and micro morphologies result in enhanced kinetic properties, which can be attributed to the effective contact between the active material and the other components of the electrode, resulting in the greatly reduced charge transfer impedance and polarization.

During the discharge process of the Mg/MnO_2 battery, the Mg electrode undergoes anodic dissolution in the electrolyte, while the MnO_2 material is converted to MnOOH by gain of electrons from the system. The electrochemical reactions involved in the Mg/MnO_2 battery can be described by the following equations [9]:

$$\text{Anode: } Mg \rightarrow Mg^{2+} + 2e^- \quad (3)$$

$$\text{Cathode: } MnO_2 + H_2O + e^- \rightarrow MnOOH + OH^- \quad (4)$$

$$\text{Overall: } Mg + 2MnO_2 + 2H_2O \rightarrow 2MnOOH + Mg^{2+} + 2OH^- \quad (5)$$

The electrochemical performances of the assembled Mg/MnO_2 CR2032 coin cells were investigated by galvanostatic discharge. Figure 6 shows the discharge curves of Mg/MnO_2 batteries made from different Mg materials. All cells were discharged at a constant current density of 25 mA/g at 25 °C. The discharge curves for samples 1, 2, and 3 displayed higher open-circuit voltages and longer flat plateaus than that of the commercial Mg powder. Sample 3 gave a plateau voltage of approximately 1.44 V and the maximum

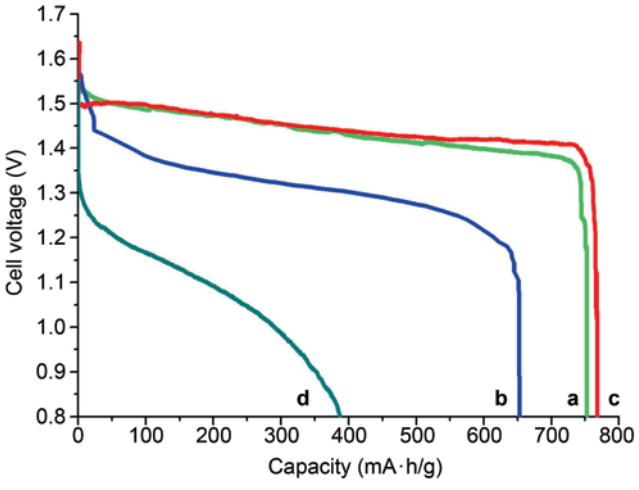

Figure 6 The discharge curves of Mg/MnO_2 batteries made from (**a**) sample 1, (**b**) sample 2, (**c**) sample 3, and (**d**) commercial Mg powder at a constant current density of 25 mA/g and a working temperature of 25 °C

discharge capacity of 768 mAh/g, showing a higher electrochemical activity than the other Mg samples. This improvement is associated with the mixed nano and micro morphologies that provide sufficient contact between the active materials in the electrode and decrease the polarization in the neutral electrolyte.

3. Conclusions

Mg microspheres and micro/nanospheres mixture have been synthesized via a conventional vapor-transport method and investigated as anode materials in Mg/MnO_2 batteries. It is found that a higher deposition temperature (300 °C) led to the formation of a Mg micro/nanoscale mixture on a stainless-steel screen mesh substrate. A mixed electrolyte of $Mg(NO_3)_2$ (2.6 mol/L) and $NaNO_2$ (2.6 mol/L) exhibited the superior properties of low corrosion rate and low anodic polarization for the Mg anode. In addition, the LSV of the electrodes indicates that the as-prepared Mg samples possessed more negative starting anodic potential and higher current densities in comparison with commercial Mg powders. Furthermore, Mg/MnO_2 batteries composed of the Mg micro/nanostructure and γ-MnO_2 nanowires displayed superior discharge performance such as long discharge plateaus and high specific discharge capacities because of the better electrochemical contact and lower electrode polarization.

Acknowledgements

This work was supported by the National 973 Program (2005CB623607), the National Natural Science Foundation of China (20873071) and Tianjin Basic & High-Tech Research (07ZCGHHZ00700 and 08JCZDJC21300).

Electronic Supplementary Material: Representative XRD pattern of γ-MnO_2 nanowires obtained via a hydrothermal method; typical XRD patterns of as-synthesized Mg at different deposition temperatures; cell parameters of Mg from Rietveld refinement compared with standard data; equivalent circuit of EIS for Mg electrodes; fitted results of R_{ct} and E_a for Mg products at different temperatures; Arrhenius plots of $\ln(T/R_{ct})$ vs $1000/T$ for different Mg samples. Supplementary material is available in the online version of this article at http://dx.doi.org/10.1007/s12274-9075-y and is accessible free of charge.

References

[1] Novák, P.; Imhof, R.; Haas, O. Magnesium insertion electrodes for rechargeable nonaqueous batteries — A competitive alternative to lithium? *Electrochim. Acta* **1999**, *45*, 351–367.

[2] Aurbach, D.; Lu, Z.; Schechter, A.; Gofer, Y.; Gizbar, H.; Turgeman, R.; Cohen, Y.; Moshkovich, M.; Levi, E. Prototype systems for rechargeable magnesium batteries. *Nature* **2000**, *407*, 724–727.

[3] Peng, B.; Liang, J.; Tao, Z. L.; Chen, J. Magnesium nanostructures for energy storage and conversion. *J. Mater. Chem.* **2009**, *19*, 2877–2883.

[4] Winter, M.; Brodd, R. J. What are batteries, fuel cells, and supercapacitors? *Chem. Rev.* **2004**, *104*, 4245–4269.

[5] Li, W. Y.; Li, C. S.; Zhou, C. Y.; Ma, H.; Chen, J. Metallic magnesium nano/mesoscale structures: Their shape-controlled preparation and Mg/air battery applications. *Angew. Chem., Int. Ed.* **2006**, *45*, 6009–6012.

[6] Kumar, G. G.; Munichandraiah, N. Ageing of magnesium/manganese dioxide primary cells. *J. Solid State Electrochem.* **2001**, *5*, 8–16.

[7] Munichandraiah, N. Electrochemical impedance studies of

a decade-aged magnesium/manganese dioxide primary cell. *J. Appl. Electrochem.* **1999**, *29*, 463–471.

[8] Renuka, R.; Ramamurthy, S. An investigation on layered birnessite type manganese oxides for battery applications. *J. Power Sources* **2000**, *87*, 144–152.

[9] Vuorilehto, K. An environmentally friendly water-activated manganese dioxide battery. *J. Appl. Electrochem.* **2003**, *33*, 15–21.

[10] Sathyanarayana, S.; Munichandraiah, N. A new magnesium-air cell for long-life applications. *J. Appl. Electrochem.* **1981**, *11*, 33–39.

[11] Cheng, F. Y.; Zhao, J. Z.; Song, W. E.; Li, C. S.; Ma, H.; Chen, J.; Shen, P. W. Facile controlled synthesis of MnO_2 nanostructures of novel shapes and their application in batteries. *Inorg. Chem.* **2006**, *45*, 2038–2044.

[12] Cheng, F. Y.; Chen, J.; Gou, X. L.; Shen, P. W. High-power alkaline Zn-MnO_2 batteries using γ-MnO_2 nanowires/nanotubes and electrolytic zinc powder. *Adv. Mater.* **2005**, *17*, 2753–2756.

[13] Tao, Z. L.; Li, C. S.; Chen, J. Mg micro/nanoscale materials with sphere-like morphologies: Size-controlled synthesis and characterization. *Sci. China Ser. G-Phys. Mech. Astron.* **2009**, *52*, 35–39.

[14] Li, W. N.; Yuan, J. K.; Shen, X. F.; Gomez-Mower, S.; Xu, L. P.; Sithambaram, S.; Aindow, M.; Suib, S. L. Hydrothermal synthesis of structure- and shape-controlled manganese oxide octahedral molecular sieve nanomaterials. *Adv. Funct. Mater.* **2006**, *16*, 1247–1253.

[15] Izumi, F.; Ikeda, T. A Rietveld-analysis program RIETAN-98 and its applications to zeolites. *Mater. Sci. Forum* **2000**, *321–324*, 198–203.

[16] Fu, L. J.; Liu, H.; Li, C.; Wu, Y. P.; Rahm, E.; Holze, R.; Wu, H. Q. Surface modifications of electrode materials for lithium ion batteries. *Solid State Sci.* **2006**, *8*, 113–128.

[17] Lee, J.; Yang, H. J.; Lee, J.; Shin, H.; Kim, J.; Jeong, C.; Cho, B.; Chung, K.; Lee, E. Adhesion, passivation, and resistivity of a Ag(Mg) gate electrode for an amorphous silicon thin-film transistor. *J. Mater. Res.* **2003**, *18*, 1441–1446.

[18] Ricci, D.; Pacchioni, G.; Sushko, P. V.; Shluger, A. L. Reactivity of $(H^+)(e^-)$ color centers at the MgO surface: Formation of O_2^- and N_2^- radical anions. *Surf. Sci.* **2003**, *542*, 293–306.

[19] Khaleel, A.; Kapoor, P. N.; Klabunde, K. J. Nanocrystalline metal oxides as new adsorbents for air purification. *Nanostruct. Mater.* **1999**, *11*, 459–468.

[20] Jarvis, L. The beneficial effect of increased cathode water content on magnesium battery performance. In *Proceedings of the 34th international power sources symposium,* Cherry Hill, New Jersey, June 25–28, 1990; Institute of Electrical and Electronics Engineers, New York, 1990; pp. 107–109.

[21] Li, C. S.; Zhang, S. Y.; Cheng, F. Y.; Ji, W. Q.; Chen, J. Porous $LiFePO_4$/NiP composite nanospheres as the cathode materials in rechargeable lithium ion batteries. *Nano Res.* **2008**, *1*, 242–248.